Supporting Information for "Muted Amazon rainfall response to deforestation in a global storm-resolving model"

Arim Yoon[1,2] *, Cathy Hohenegger[1]

[1]Max Planck Insititute for Meteorology

[2]International Max Planck Research School on Earth System Modeling (IMPRS-ESM)

Contents of this file

1. Figures S1 to S7
2. Tables S1 to S3

Introduction This Supporting Information contains figures and tables that support the manuscript. It includes figures to evaluate the design of the simulation and its performance against observations as well as analyses to help understand the climate patterns of the intact Amazon. It also includes additional figures showing changes in vertical circulation and precipitation after deforestation including May and June. A table showing the values of land surface biophysical parameters for the deforestation scenario is included. There are also two tables summarising the available GCM and RCM studies.

---

*Max Planck Insititute for Meteorology

References

Correia, F. W. S., Alvalá, R. C. d. S., & Manzi, A. O. (2008). Modeling the impacts of land cover change in amazonia: a regional climate model (rcm) simulation study. *Theoretical and Applied Climatology*, *93*, 225–244.

Costa, M. H., & Foley, J. A. (2000). Combined effects of deforestation and doubled atmospheric co 2 concentrations on the climate of amazonia. *Journal of Climate*, *13*(1), 18–34.

Da Silva, R. R., Werth, D., & Avissar, R. (2008). Regional impacts of future land-cover changes on the amazon basin wet-season climate. *Journal of climate*, *21*(6), 1153–1170.

Dickinson, R. E., & Kennedy, P. (1992). Impacts on regional climate of amazon deforestation. *Geophysical Research Letters*, *19*(19), 1947–1950.

Dirmeyer, P. A., & Shukla, J. (1994). Albedo as a modulator of climate response to tropical deforestation. *Journal of Geophysical Research: Atmospheres*, *99*(D10), 20863–20877.

Gandu, A. W., Cohen, J. C. P., & De Souza, J. (2004). Simulation of deforestation in eastern amazonia using a high-resolution model. *Theoretical and Applied Climatology*, *78*, 123–135.

Gedney, N., & Valdes, P. J. (2000). The effect of amazonian deforestation on the northern hemisphere circulation and climate. *Geophysical Research Letters*, *27*(19), 3053–3056.

Hahmann, A. N., & Dickinson, R. E. (1997). Rccm2–bats model over tropical south america: Applications to tropical deforestation. *Journal of Climate*, *10*(8), 1944–1964.

Hirota, M., Oyama, M. D., & Nobre, C. (2011). Concurrent climate impacts of tropical

south america land-cover change. *Atmospheric Science Letters*, *12*(3), 261–267.

Kleidon, A., & Heimann, M. (2000). Assessing the role of deep rooted vegetation in the climate system with model simulations: mechanism, comparison to observations and implications for amazonian deforestation. *Climate Dynamics*, *16*, 183–199.

Lean, J., & Rowntree, P. (1993). A gcm simulation of the impact of amazonian deforestation on climate using an improved canopy representation. *Quarterly Journal of the Royal Meteorological Society*, *119*(511), 509–530.

Lean, J., & Rowntree, P. (1997). Understanding the sensitivity of a gcm simulation of amazonian deforestation to the specification of vegetation and soil characteristics. *Journal of Climate*, *10*(6), 1216–1235.

Lean, J., & Warrilow, D. A. (1989). Simulation of the regional climatic impact of amazon deforestation. *Nature*, *342*(6248), 411–413.

Lejeune, Q., Davin, E. L., Guillod, B. P., & Seneviratne, S. I. (2015). Influence of amazonian deforestation on the future evolution of regional surface fluxes, circulation, surface temperature and precipitation. *Climate Dynamics*, *44*, 2769–2786.

Llopart, M., Reboita, M. S., Coppola, E., Giorgi, F., Da Rocha, R. P., & De Souza, D. O. (2018). Land use change over the amazon forest and its impact on the local climate. *Water*, *10*(2), 149.

Medvigy, D., Walko, R. L., & Avissar, R. (2011). Effects of deforestation on spatiotemporal distributions of precipitation in south america. *Journal of Climate*, *24*(8), 2147–2163.

Moore, N., Arima, E., Walker, R., & Ramos da Silva, R. (2007). Uncertainty and the

changing hydroclimatology of the amazon. *Geophysical Research Letters*, *34*(14).

Nobre, C. A., Sellers, P. J., & Shukla, J. (1991). Amazonian deforestation and regional climate change. *Journal of climate*, *4*(10), 957–988.

Nobre, P., Malagutti, M., Urbano, D. F., de Almeida, R. A., & Giarolla, E. (2009). Amazon deforestation and climate change in a coupled model simulation. *Journal of Climate*, *22*(21), 5686–5697.

Pires, G. F., & Costa, M. H. (2013). Deforestation causes different subregional effects on the amazon bioclimatic equilibrium. *Geophysical Research Letters*, *40*(14), 3618–3623.

Segura, H., Hohenegger, C., Wengel, C., & Stevens, B. (2022). Learning by doing: Seasonal and diurnal features of tropical precipitation in a global-coupled storm-resolving model. *Geophysical Research Letters*, *49*(24), e2022GL101796.

Spracklen, D., & Garcia-Carreras, L. (2015). The impact of amazonian deforestation on amazon basin rainfall. *Geophysical Research Letters*, *42*(21), 9546–9552.

Werth, D., & Avissar, R. (2002). The local and global effects of amazon deforestation. *Journal of Geophysical Research: Atmospheres*, *107*(D20), LBA–55.

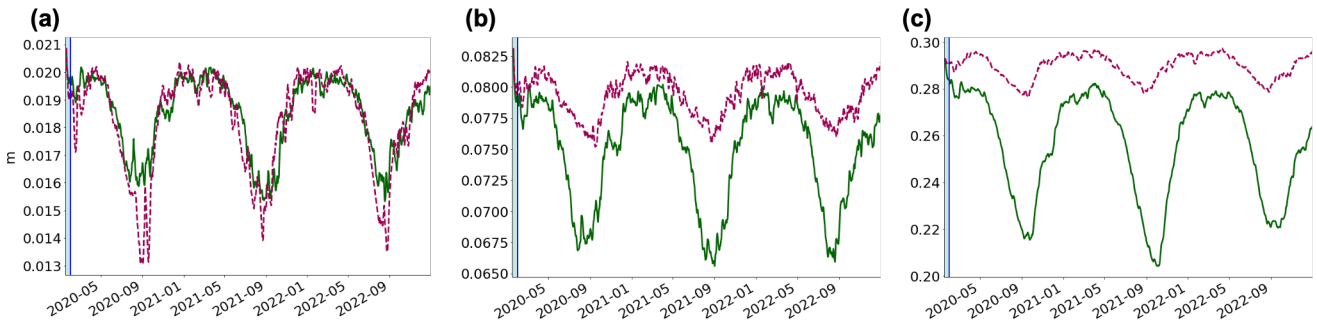

Figure S1. Daily averaged soil moisture [m] in the (a) 1st (0-0.065m), (b) 2nd (0.065-0.384m) and (c) 3rd (0.384-1.551m) soil layer for CTL (solid green) and DEF (dashed magenta). Only the first three soil layers are hydrologically active over the Amazon region, layers 4 and 5 are bedrock. Blue coloring highlights the discarded spin-up period (i.e., January 2020).

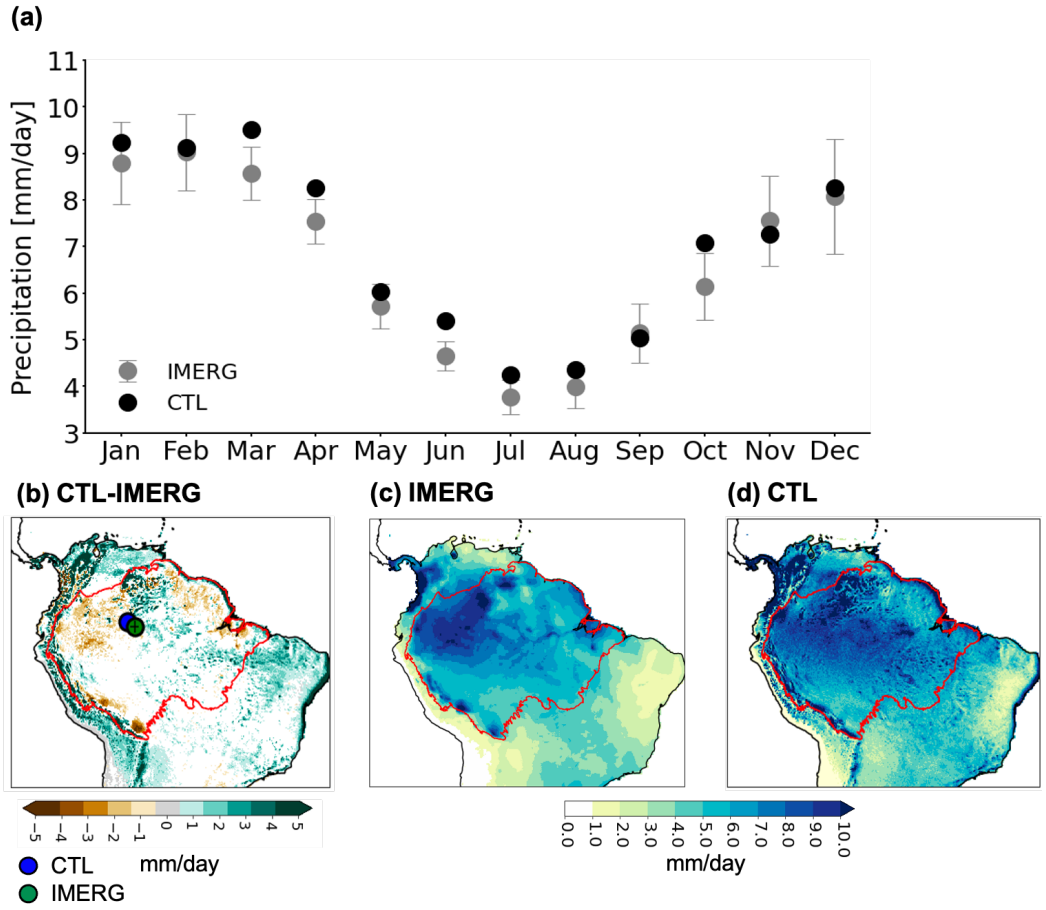

Figure S2. (a) Monthly mean precipitation over the Amazon region indicated with red boundary in Fig. b from 3-y averaged CTL and 20-y averaged observations from IMERG (2001-2021). IMERG is plotted with interannual variability (standard deviation). (b) Map of the difference of the annual mean precipitation (CTL-IMERG). If the difference in precipitation is smaller than the standard deviation of IMERG, the value is masked out and colored in white. The yearly mean location of the weighted centroid of the rainbelt over South America is added with blue (ICON) and green (IMERG) dots (see Methods). The IMERG dot is shown with its interannual variability in latitude and longitude indicated by the bars. Maps of the annual mean of precipitation (mm day^{-1}) in (c) IMERG and (d) CTL. All maps are in 82°W-30°W and 30°S-13°N over land only.

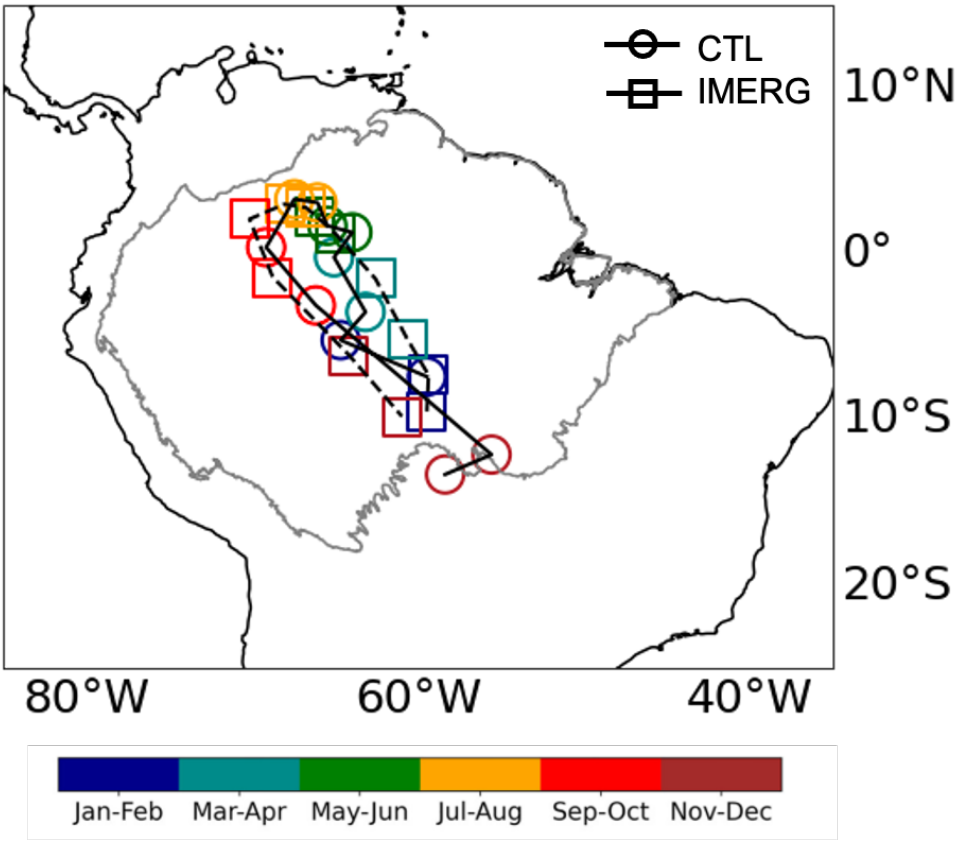

Figure S3. Seasonal migration of the monthly mean location of the centroid of the rainbelt over South America (82°W–30°W; 30°S–13°N) calculated by using the SAL method for CTL (circles and solid lines) and IMERG (squares and dashed lines). Marker colors indicate the month and for a better visualization, colors are grouped by 2 months. See Segura et al. (2022) for more detail.

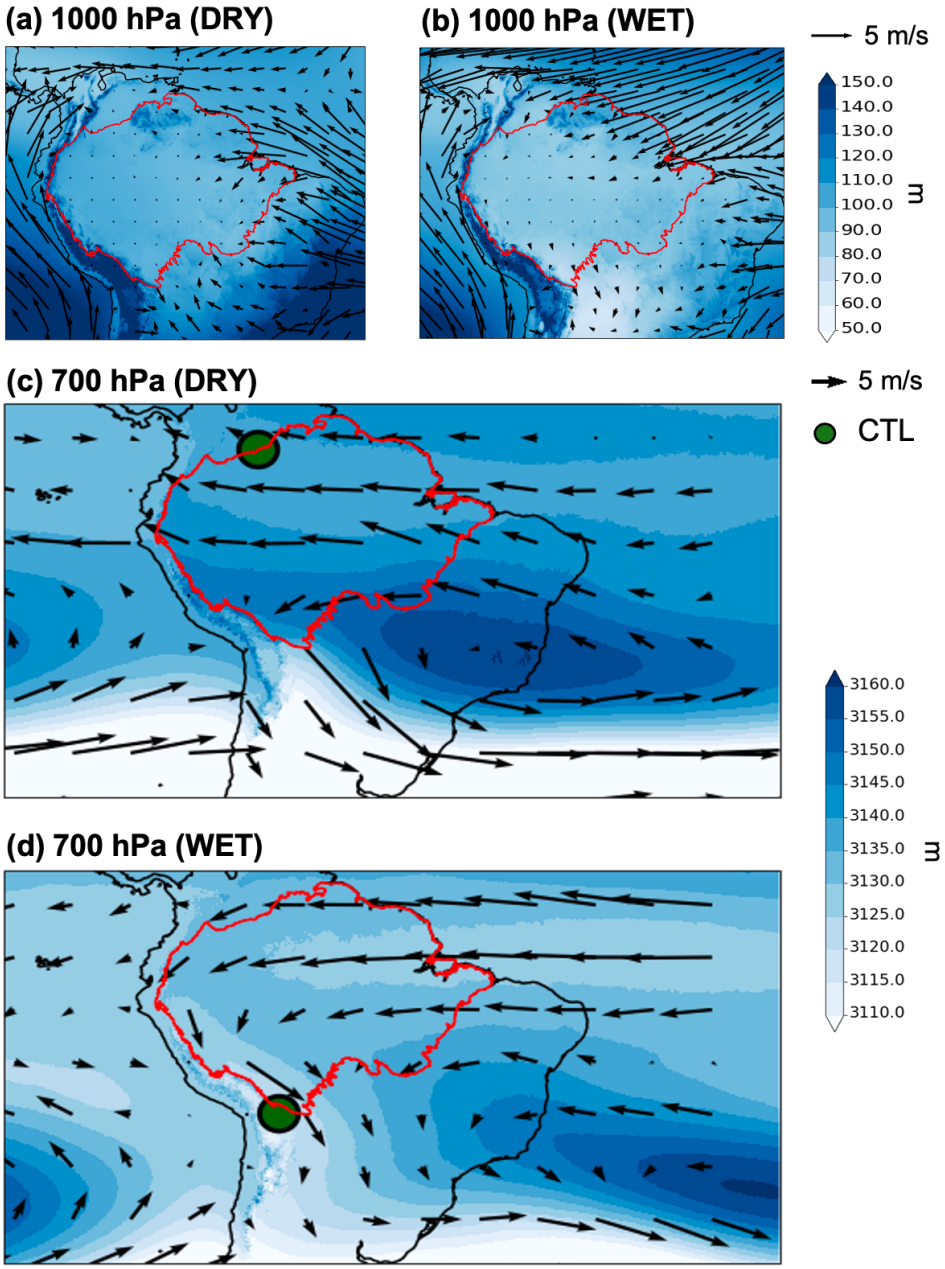

Figure S4. Maps of geopotential height (shading) and wind (arrow) at the 1000 hPa in CTL during (a) dry (JAS) and (b) wet (DJF) seasons. The corresponding distribution of geopotential height and wind at the 700-hPa level in CTL is shown in (c) for the dry and (d) wet seasons. Green circle for the location of the center of the rainbelt.

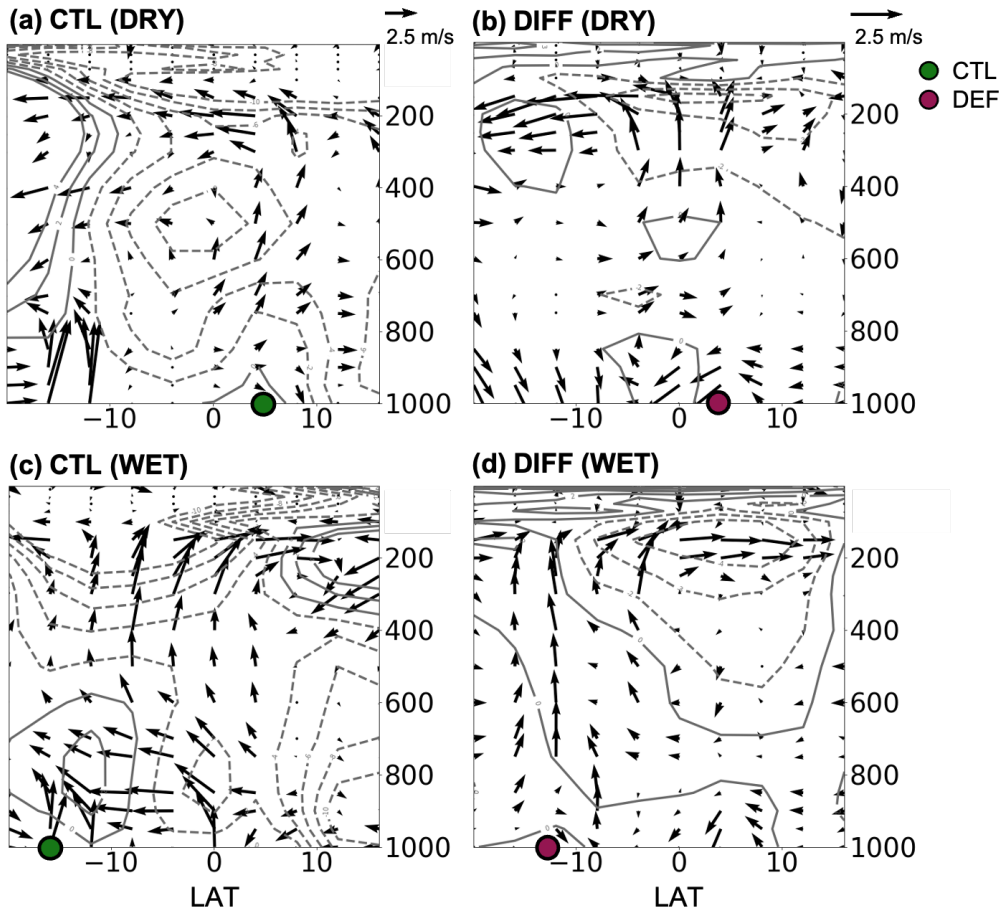

Figure S5. The vertical profile of zonally averaged wind over domain 20°S-20°N, 80°W-60°W. The meridional and vertical wind is plotted with arrows and the zonal wind is plotted with lines (solid positive, dashed negative). The filled circles (CTL: dark green, DEF: dark magenta) represent the latitude of the center of the rainbelt.

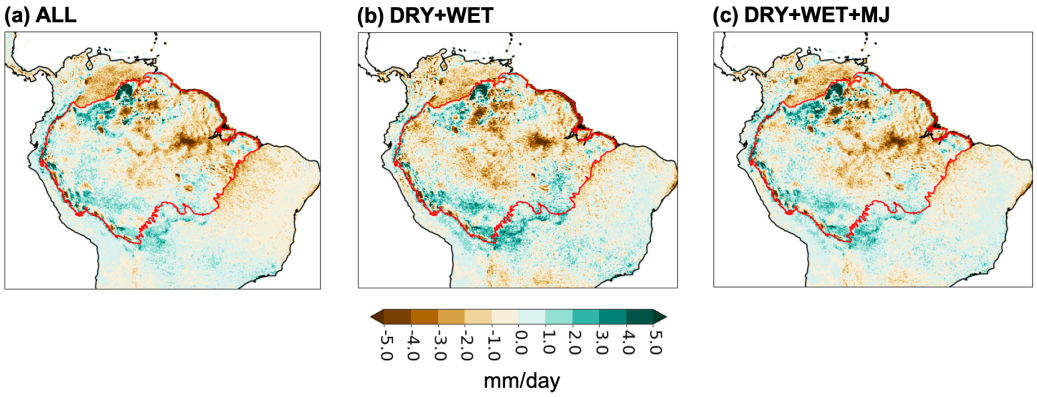

Figure S6. Maps of changes in precipitation (mm day^{-1}, DEF-CTL) averaged over the (a) whole period, (b) dry (JAS) and wet (DJF), and (c) dry (JAS), wet (DJF) and transitional (May, June) period.

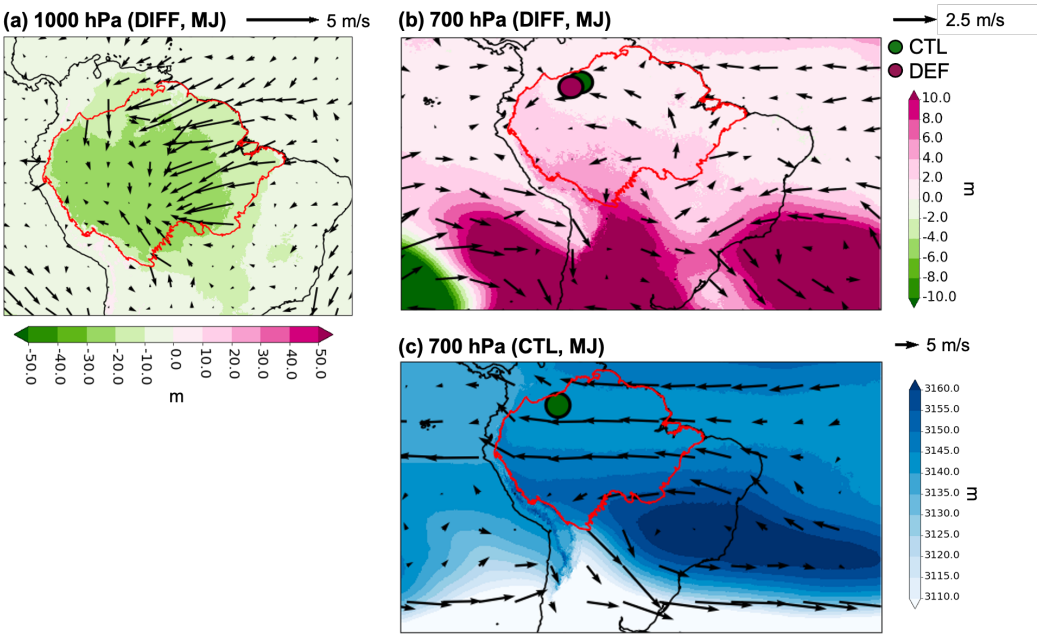

Figure S7. (a) Maps of changes (DEF-CTL) in geopotential height (shading) and wind (arrow) at the 1000 hPa. (b) shows the corresponding situation at 700 hPa with filled circles for the location of the rainbelt center. The mean circulation at 700 hPa together with the geopotential height in CTL only is shown in panel (c). All panels as averages over May and June.

Table S1. The GCMs and land surface scheme, resolution, and the use of an ocean model (A for atmosphere-only, C for coupled-ocean-atmosphere) are indicated together with the resulting spatial pattern of the precipitation change, the change in the annual mean evapotranspiration (ET, mm day^{-1}) and precipitation (P, mm day^{-1} and %). The average precipitation reduction from past GCM studies is 1.05 mm/day (17.82%). For the spatial pattern, the first cardinal direction has more precipitation after deforestation (e.g., E/W = East becomes wetter and west becomes drier after deforestation), and '-' is used if there is no mention of spatial pattern. The format is similar to the supplementary table from Spracklen & Garcia-Carreras (2015). *Hirota et al (2011) showed a similar pattern to our study, but no detail about the underlying mechanism can be found.

Reference	Model	Resolution	Ocean	Pattern	ET	P (%)
Lean & Warrilow (1989)	UKMO	2.5×3.75	A	-	-0.85	-1.34 (-20)
C. A. Nobre et al. (1991)	NMC/SiB	1.8×2.8	A	Uniform	-1.43	-1.76 (-26.1)
Dickinson & Kennedy (1992)	NCAR CCM1 BATS	4×7.5	A	-	-0.7	-1.4 (-25.5)
Lean & Rowntree (1993)	UKMO	2.81×2.81	A	Uniform	-0.55	-0.81 (-14.2)
Dirmeyer & Shukla (1994)	COLA/SSiB	4.5×7.5	A	NE/SW	-0.33	-0.28 (-11.4)
Lean & Rowntree (1997)	UKMO	2.5×3.75	A	Uniform	-0.3	-0.3 (-5)
Hahmann & Dickinson (1997)	NCAR CCM2 BATS1e	2.81×2.81	C	E/W	-0.41	-0.99 (-16.6)
Costa & Foley (2000)	GENESIS IBIS	4.5×7.5	C	S/N (JFM,JAS)	-0.61	-0.73 (-11.8)
Gedney & Valdes (2000)	ECMWF IFS	3×3	C	-	-0.65	-0.79 (-15.6)
Kleidon & Heimann (2000)	ECHAM4	5.6×5.6	A	E/W	-1.30	-0.38 (-7.7)
Werth & Avissar (2002)	GISS-II	4×5	A	-	-0.59	-0.81 (-21.7)
Da Silva et al. (2008)	GISS	5×4	A	Uniform (JF)	-0.71	-1.25 (-19.0)
P. Nobre et al. (2009)	CPETC SSiB	1.85×2.85	C	E/W	-	-3.3 (-42)
Medvigy et al. (2011)	OLAM	Variable, 25km over Amazon	A	SE/NW	-0.04	-0.17 (-2.3)
Hirota et al. (2011)	CPTEC	1×1	A	W/E*	-	-1.38 (-27.6)
Pires & Costa (2013)	CCM3/IBIS	2.81×2.81	A	-	-	-1.15 (-18.6)

Table S2. Same as Table S1 but for RCM studies. The average decrease in precipitation is 0.60 mm day^{-1} (7.88%). *Correia et al. (2008) showed a significant precipitation decrease in the eastern and northeastern Amazon and a narrow increase in the extreme western part along the Andes. Compared to our obtained spatial pattern, they miss the increase over the northern and southern Amazon and their increase over the western Amazon is narrower.

Reference	Model	Resolution	Ocean	Pattern	ET	P (%)
Moore et al. (2007)	RAMS4.4	20 km	A	Band (E to W)	-	-0.41 (-8.2)
Da Silva et al. (2008)	RAMS	20 km	A	E/W	-0.88	-1.00 (-12.5)
Correia et al. (2008)	ETA/SSiB	40 km	A	W/E*	-1.28	-1.29 (-12.6)
Lejeune et al. (2015)	COSMO-CLM	0.44×0.44	A	E/W	-0.4	-0.22 (-5.3)
Llopart et al. (2018)	RegCM4/CLM4.5	50 km	A	E/W	-0.55	-0.06 (-0.8)

Table S3. The values for the forest are an average of the grid point values from JSBACH over the Amazon and the values for pasture are taken from a table in Gandu et al. (2004), which based their values on multiple previous studies. The value for the root depth is from Correia et al. (2008), as this gives a larger difference to the forest case given the small root depth of the forest in JSBACH (1.3 m against 4.0 m in Gandu et al. (2004)). The table only includes the values of the parameters that we directly changed, not all the parameters that could potentially be changed by these changes such as stomal conductance.

Parameters	Forest $\rightarrow$ Pasture
Albedo	0.12 $\rightarrow$ 0.18
Leaf Area Index	8.40 $\rightarrow$ 2.70
Vegetation fraction	0.92 $\rightarrow$ 0.85
Roughness length (m)	1.80 $\rightarrow$ 0.05
Root depth (m)	1.33 $\rightarrow$ 0.60
Forest fraction	0.86 $\rightarrow$ 0.00